

Are your MRI contrast agents cost-effective?

Learn more about generic Gadolinium-Based Contrast Agents.



FRESENIUS
KABI

caring for life

AJNR

Differential aging of the human striatum: a prospective MR imaging study.

F M Gunning-Dixon, D Head, J McQuain, J D Acker and N Raz

AJNR Am J Neuroradiol 1998, 19 (8) 1501-1507

<http://www.ajnr.org/content/19/8/1501>

This information is current as of April 16, 2024.

Differential Aging of the Human Striatum: A Prospective MR Imaging Study

Faith M. Gunning-Dixon, Denise Head, John McQuain, James D. Acker, and Naftali Raz

BACKGROUND AND PURPOSE: Advancing age is associated with declines in motor function; understanding age-related changes in the basal ganglia, therefore, is imperative for comprehension of such functional changes. The purpose of this study was to examine the age, sex, and hemispheric differences in volume of the caudate nucleus, the putamen, and the globus pallidus.

METHODS: In a sample of 148 healthy right-handed adults (18–77 years old) with no evidence of age-related motor disorders, we estimated the volume of the head of the caudate nucleus, the putamen, and the globus pallidus from MR images.

RESULTS: The analyses revealed bilateral age-related shrinkage of the head of the caudate nucleus and the putamen in both sexes. In men, the age-related shrinkage of the caudate was stronger on the left, whereas, in women, the opposite trend was evident. In both sexes, age-related shrinkage of the right putamen was greater than of its left counterpart. The mild bilateral age-related shrinkage of the globus pallidus was observed only in men. In both sexes, we observed significant rightward asymmetry in the putamen, significant leftward asymmetry in the caudate, and no asymmetry in the globus pallidus.

CONCLUSIONS: Bilateral age-related shrinkage of the neostriatum is found in healthy adults. The shrinkage of the globus pallidus is less pronounced and may be restricted to men only.

The basal ganglia are widely believed to be the neural substrate of the planning, execution, and control of movement in vertebrates (1). Because these functions decline with advancing age (2, 3), an understanding of the course and the mechanisms of age-related changes in the basal ganglia is critical for the comprehension and possible remediation of functional deficits. Although the literature reports moderate age-related shrinkage in both the caudate nucleus (median correlation with age, $r = -.49$) and the putamen (median, $r = -.52$), the relationship between age and the globus pallidus has received little attention (4).

Motor activity is not only susceptible to age-related

changes but differs across the sexes as well (5). These differences may reflect gender-related variations in striatal volume, although the sparse published data suggest no sex-related volumetric differences in the neostriatal nuclei (4). In two previous studies (4), we found a slightly steeper age-related decline of the caudate volume in men than women, whereas age-related shrinkage of the putamen was found in men only. Another source of variability in motor behavior is lateral asymmetry (6). A recent quantitative review (4) revealed little consistency across the samples in measures of striatal asymmetry. Although leftward asymmetry of the globus pallidus is common, the evidence of hemispheric differences in the neostriatum is equivocal. The objectives of the present study were to determine whether specific basal ganglia age differentially and to examine the effects of sex and hemispheric differences on each of the ganglia in a life span sample of healthy adults.

Methods

Subjects

The data for this study were collected in an ongoing investigation of neuroanatomic correlates of age-related differences in cognition. The participants consisted of healthy adults recruited by advertising in local media and on the University of Memphis campus. Consent forms were signed by the subjects and approved by the Committee for Protection of Human Subjects in Research of the University of Memphis and by the

Received September 30, 1997; accepted after revision April 3, 1998.

Supported in part by the National Institutes of Health grant AG-11230 (N.R.) and by the Center of Excellence Grant from the State of Tennessee to the Department of Psychology, University of Memphis.

Presented in part at the annual meeting of the Society for Neuroscience, San Diego, CA, November 1995, and at the annual meeting of the Society for Neuroscience, Washington, DC, November 1996.

From the Department of Psychology, the University of Memphis (F.M.G.-D., D.H., J.M., N.R.); and Baptist MRI, Baptist Memorial Hospital-East, Memphis (J.D.A.).

Address reprint requests to Naftali Raz, PhD, Department of Psychology, University of Memphis, Memphis, TN 38152.

Baptist Memorial Hospital Patients Participation Committee. Subjects were screened by means of an extensive health questionnaire. Persons who reported a history of cardiovascular, neurologic, and psychiatric conditions, head trauma with loss of consciousness for more than 5 minutes, thyroid dysfunction and diabetes, treatment for drug and alcohol problems, or a habit of taking more than three alcoholic drinks per day were excluded from the study. None of the subjects used antiseizure medication, anxiolytics, or antidepressants. Of 166 subjects who underwent MR imaging, all or substantial portions of the data for eight subjects were lost because of technical problems, such as disk failure, excessive movement artifacts, operator error, and (in two cases) significant discomfort of the subject during scanning.

All subjects were screened for dementia and depression by using a modified Blessed Information-Memory-Concentration Test (7) with a cutoff score of 30 and the Geriatric Depression Questionnaire (8) with a cutoff score of 15. Finally, the MR images of all subjects admitted to the study (see below for the details of image acquisition) were examined by an experienced neuroradiologist. Neuroradiologic signs of mild to moderate cerebrovascular disease commonly used in clinical practice were used in this screening process. These signs included the presence of lacunar infarcts in the basal ganglia and the brain stem, numerous punctate lesions, and significant unilateral concentration of white matter hyperintensities, including irregular periventricular hyperintensities but excluding minimal periventricular caps. This clinical classification corresponds to grades 1 to 3 of some frequently used rating schemes (9). After the examination, 10 subjects (six men and four women, all older than 65 years of age) were removed from the sample because of mild to moderate cerebrovascular disease. The aspect of the process most relevant to this study was the exclusion of subjects in whom basal ganglia hyperintensities were detected on T2-weighted images. On the spoiled gradient-recalled acquisition (SPGR) T1-weighted images, we identified several cases of hypointensities in all three nuclei, especially in the globus pallidus. These hypointense spots, in the absence of the hyperintensities on the T2-weighted images, most likely reflected calcification and accumulation of iron, processes whose clinical and pathologic significance is unclear. The pallidal iron deposits that are absent on infants' and children's MR images appear in young adults and reach their asymptotic concentration in the third decade of life (10). Although the subjects in whom basal ganglia hypointensities were detected ($n = 54$, or 36.5% of the total sample) were significantly older than those who had none (mean age, 53.7 ± 15.1 years vs 42.2 ± 16.7 years; $t = 4.11$; $P < .001$), we retained these subjects in the sample in the absence of reports associating this finding with clinical and pathologic findings. Twelve subjects (five men and seven women) with hypertension were also retained, because their blood pressure was successfully controlled by medication. Screening of the MR images for vascular lesions greatly reduced the possibility that hypertension may have been a confound in the volumetric findings, because blood pressure is predictive of the volume of the white matter lesions only in subjects with very substantial white matter hyperintensities (11).

The final sample consisted of 148 healthy adults with an age range of 18 to 77 years (mean age, 46.5 ± 17.2 years). The subjects included 66 men (mean age, 47.4 ± 18.1 years) and 82 women (mean age, 45.7 ± 16.5 years), with no differences in age between the sexes ($t[146] = .59$). All subjects were strongly right-handed, as measured by the Edinburgh Handedness Questionnaire (12). The results pertaining to age-related differences in the cerebral cortex and the cerebellum observed in this sample or its part have been previously reported (13, 14).

MR Image Acquisition and Processing

Volume images were acquired on a 1.5-T scanner using T1-weighted 3D SPGR sequences. For each subject, 124 contiguous axial sections were acquired with imaging parameters

of 24/5 (TR/TE), a section thickness of 1.3 mm, and a flip angle of 30°. After the SPGR sequence, a fast spin-echo sequence of interleaved T2- and proton density-weighted axial images was acquired to be used in screening for age-related cerebrovascular disease. In this sequence, the parameters were 3300/90 for T2-weighted sections and 3300/18 for proton density-weighted sections. Section thickness was 5 mm, with an intersection gap of 1.5 mm.

After acquisition, the SPGR images were reformatted offline in order to correct the image for the undesirable effects of head tilt, pitch, and rotation. Standard neuroanatomic landmarks were used to bring each brain into a unified system of coordinates and to correct deviations in all three orthogonal planes. In this standard position, the sagittal plane cut through the middle of the interhemispheric fissure. The axial plane passed through the anterior and posterior commissures (incorporating the anterior commissure-posterior commissure line) and through the orbits, perpendicular to the sagittal plane. The coronal plane was leveled by the orbits and the auditory canals and passed perpendicular to the axial plane. Reformatted images were cut into sections 1.5 mm apart in the coronal plane and saved on a VHS tape. Thickness of the reformatted section was 0.86 mm (one linear pixel).

Morphometry was performed on a PC-based system. Each image was displayed on a 27-inch video monitor screen with standard brightness and contrast, and outlined regions of interest (ROIs) were traced manually using a digitizing tablet. The areas of the ROIs were computed by Java software, and the volumes of the ROIs were calculated using the basic volume estimate (15), which is a sum of the ROIs multiplied by the intersection distance. All measures were calibrated using a standard ruler bar provided on the MR images, and volumes were computed in cubic centimeters (cm^3).

Delineation of the ROIs

Three trained operators who were blinded to the subjects' exact age and sex manually traced all ROIs. The sections containing each ROI were randomly divided into two equal groups, so that each half-sample was traced by a different operator. Interrater reliability of the volume estimates was assessed by intraclass correlations for two fixed raters (16). Reliability among all pairs of the three trained operators exceeded .95 for both the caudate nucleus and the putamen, whereas the reliability in a subset of two operators for tracing of the globus pallidus was an intraclass correlation of .98. All questionable cases were resolved by consulting the correlative images and general brain atlases (17-19).

Caudate Nucleus.—The volume of the head and the body of the caudate nucleus was estimated from 15 to 20 coronal sections. The most rostral section was the one on which the caudate first appeared, usually lateral to the lateral ventricles. The caudate was traced on every other section (intersection distance, 3 mm) until no longer visible. The caudate was bordered by the lateral ventricle medially, by the internal capsule laterally, and by white matter dorsally. On the rostral sections, the ventral boundary consisted of the stria terminalis. On more anterior sections of the caudate nucleus, the septal nucleus served as the ventral border. Because the transition between the caudate nucleus and the septal nucleus was often difficult to determine, the ventral border was defined as a line drawn from the most ventral part of the internal capsule to the most ventral part of the lateral ventricle. An example of caudate nucleus tracing is presented in Figure 1.

Putamen.—The volume of the putamen was estimated from 15 to 20 coronal sections. We began tracing on the most rostral section on which the putamen was visible and continued to the most caudal section on which it could be detected. The external capsule demarcated the putamen laterally throughout the ROI. The dorsal boundary of the putamen was white matter. The internal capsule delineated the medial border until the anterior commissure was reached. At this point, the globus pallidus

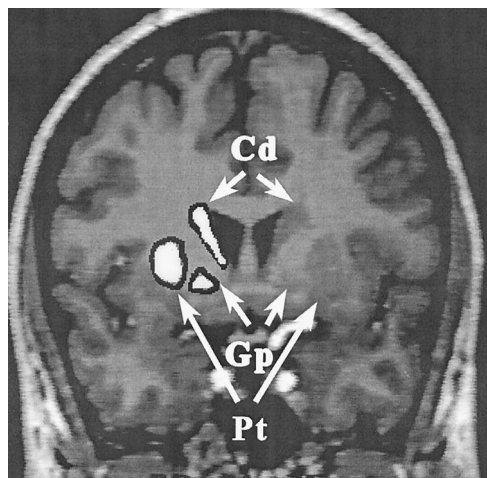


FIG 1. A typical coronal MR image with the head of the caudate nucleus (Cd), the putamen (Pt), and the globus pallidus (Gp) highlighted.

became the medial border of the putamen. The temporal stem, optic radiations, amygdala, temporal horn, and anterior commissure served as the ventral boundary of the putamen. The putamen was measured on every other section (intersection distance, 3 mm) until it was no longer visible. An example of the putamen tracing is presented in Figure 1.

Globus Pallidus.—Because of the poor resolution of the most rostral regions of the globus pallidus, we began measuring this structure on the section on which the anterior commissure was present. The globus pallidus was measured on six to seven continuous coronal sections (intersection distance, 1.5 mm). Thus, the voxel size for the pallidal measures was 1.11 cm³ (half that of the caudate and the putamen). The putamen demarcated the lateral border of the globus pallidus, and the internal capsule defined the medial border. On the most rostral sections of the globus pallidus, the ventral boundary was the anterior commissure. On the more caudal sections, the ventral border consisted of the preoptic and olfactory areas. The appearance of the mammillary bodies marked the most caudal section. Figure 1 displays an example of the tracing of the globus pallidus.

Results

The descriptive statistics for the volumes of three striatal nuclei in both hemispheres are presented in Table 1. The results for each gender group are presented along with those for the total sample.

The effects of age, sex, and hemisphere on the volumes of the striatal nuclei were tested within a general linear model framework. First, we fitted the data to a multivariate analysis of the covariance model, in which the volumes of each hemisphere of

each striatal nucleus formed a vector of dependent variables, gender was a grouping factor, age was a continuous independent variable, and height was a covariate. The continuous independent variable and the covariate (height) were recentered at their respective means. The full model, including the interactions between each continuous variable and the grouping factor, was tested to check for the homogeneity of regression slopes across groups. The model failed the homogeneity of regression slopes test, yielding a significant nucleus × height interaction (Wilks' $\Lambda = .92$, $F[2, 141] = 6.07$, $P < .01$). Thus, the adjustment for differences in body size that was needed for comparison between the sexes could not be performed using the same regression for all striatal components and separate models were fitted for each nucleus. Within the full model, however, in addition to the expected volume difference among the structures (Wilks' $\Lambda = .04$, $F[2, 141] = 1820.38$, $P < .001$), a significant age × nucleus interaction (Wilks' $\Lambda = .79$, $F[2, 141] = 18.34$, $P < .001$) was present, indicating that the effects of age on the volume of striatal components were not uniform. The overall effect of age on the striatal volume was significant ($F[1, 142] = 40.24$, $P < .001$). In addition, a significant hemisphere × nucleus interaction (Wilks' $\Lambda = .58$, $F[2, 141] = 51.97$, $P < .001$) indicated significant variation in the pattern of hemispheric differences across the basal ganglia.

To examine the effects of sex, age, and hemisphere on each striatal component while taking into account differences in body size (stature), we fitted the data to three univariate linear models. In these three mixed linear models, the homogeneity of regression slopes across the groups was again tested by including all the interactions. If these interactions were nonsignificant, they were removed from the model, and the reduced model was fitted to the data. Hemisphere was treated as a repeated measure. The results of these analyses are presented below for each striatal component separately (Fig 2).

Caudate Nucleus

Interactions of continuous variables with height were not significant ($P > .10$) and were dropped from the model. The significant main effect of age on the caudate nucleus ($F[1, 143] = 19.00$, $P < .001$) was modified by the significant age × sex × hemisphere interaction ($F[1, 143] = 5.84$, $P < .02$). As indicated by standardized regression coefficients after adjust-

TABLE 1: Descriptive statistics for the volumetric measures of the basal ganglia*

	Total Sample						Women						Men					
	Caudate Nucleus		Putamen		Globus Pallidus		Caudate Nucleus		Putamen		Globus Pallidus		Caudate Nucleus		Putamen		Globus Pallidus	
	R	L	R	L	R	L	R	L	R	L	R	L	R	L	R	L	R	L
Mean	3.34	3.43	4.36	4.02	.82	.81	3.26	3.34	4.19	3.88	.79	.79	3.44	3.53	4.56	4.18	.84	.84
SD	.52	.54	.61	.60	.10	.10	.44	.49	.53	.54	.10	.10	.59	.58	.64	.62	.09	.09

* All volumes are in cm³.

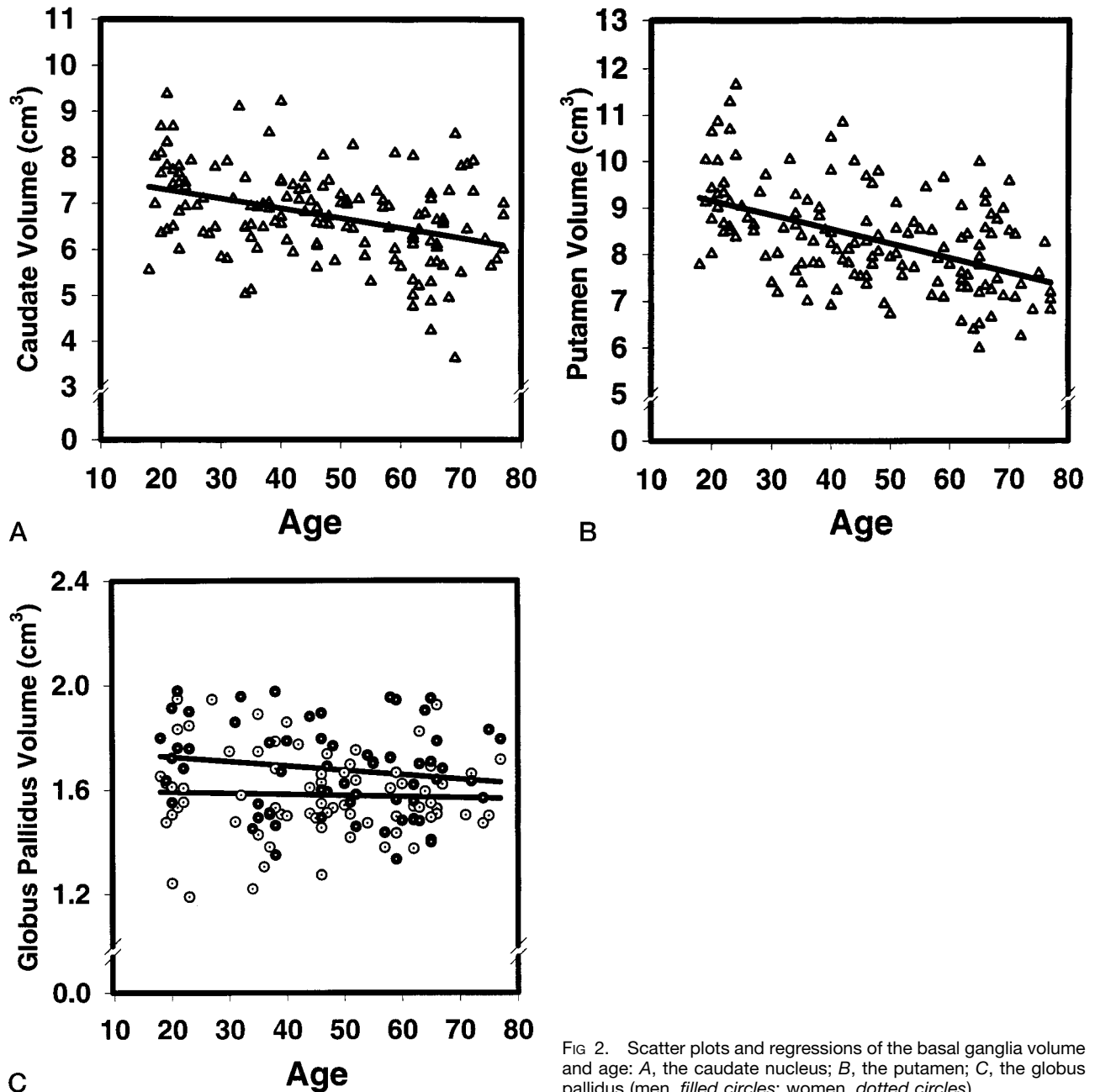


FIG 2. Scatter plots and regressions of the basal ganglia volume and age: A, the caudate nucleus; B, the putamen; C, the globus pallidus (men, filled circles; women, dotted circles).

ment for height, somewhat greater age-related shrinkage of the left versus the right caudate nucleus ($\beta = -.41$ vs $\beta = -.27$) was evidenced in men, whereas a trend in the opposite direction ($\beta = -.26$ vs $\beta = -.37$) was revealed in women. For both sexes, the left caudate volume was greater than the right (3.43 vs 3.34 cm³; $F[1, 135] = 14.12$, $P < .001$, an asymmetry of 2.66%). (The index of hemispheric asymmetry was computed as the absolute percentage difference: $100\% \times [(left - right)/\frac{1}{2}(left + right)]$.) The estimated average rate of caudate shrinkage at a span between 20 and 80 years of age was 3.3% per decade. The estimated shrinkage rates by sex and hemisphere were 4.0% and 2.9% for the left and right caudate, respectively, in men, and 2.5% and 3.3% for the corresponding nuclei in women.

Putamen

All the interactions between sex and continuous variables were not significant, and the effects of age, sex, and hemisphere on the volume of the putamen were examined in a reduced model. The analysis revealed a significant main effect of age ($F[1, 144] = 38.27$, $P < .001$). Greater aging was noted in the right than in the left putamen ($F[1, 144] = 5.53$, $P < .02$). Additionally, the right putamen was larger than the left one (4.36 vs 4.02 cm³; $F[1, 144] = 192.26$, $P < .001$). The magnitude of this rightward asymmetry (8.17%) was stronger than that of the leftward bias in the volume of the caudate nucleus. The observed shrinkage of the whole putamen corresponds to the rate of approximately 3.6% per decade within a span

TABLE 2: Correlations among striatal volumes, height, and age

	Total Sample				Women				Men			
	Cd	Pt	Gp	Age	Cd	Pt	Gp	Age	Cd	Pt	Gp	Age
Height	.20*	.37***	.28***	.05	.02	.22	.10	.05	.19	.30**	.15	.00
Caudate nucleus		.53***	.17*	-.32***		.48***	.10	-.32**		.54***	.16	-.35**
Putamen			.16*	-.41***			-.03	-.43***			.23	-.45***
Globus pallidus				-.10				.06				-.33**

* $P < .05$; ** $P < .01$; *** $P < .001$.

Note.—All volumes are summed across two hemispheres.

of 20 to 80 years of age, with the estimates for the right and the left putamen standing at 3.7% and 3.2%, respectively.

Globus Pallidus

The interaction between sex and height was not significant and was dropped from the model. Although age was not a main effect ($F[1, 143] = 2.05$), a significant age \times sex interaction ($F[1, 143] = 5.41$, $P < .03$) was present. Decomposition of this interaction revealed that significant age-related shrinkage of the globus pallidus was restricted to men only ($\beta = -.33$ vs $\beta = .06$ for men and women, respectively). No hemispheric differences in pallidal volume for either sex were noted. The estimated rate of globus pallidus shrinkage for men was 1.9% per decade.

Differential Aging of the Striatum in Men and Women

We compared the magnitude of age effects on each striatal nucleus by using zero-order correlations between age and ROI volumes (Table 2). In this comparison we used Steiger's Z^* statistic, which takes into account the correlation between the variables correlated with age (20). For women, the correlation between putamen volume and age and caudate volume and age was significantly larger than the correlation between globus pallidus volume and age ($Z^* = 3.18$, $P < .001$ and 2.63 , $P < .01$, respectively). The correlations of the neostriatal volumes with age did not differ significantly ($Z^* = .98$). For men, the negative association between age and the volume of all three basal ganglia was equally strong (all Z^* scores were < 1.12 and were not significant).

Discussion

The results of the study provide evidence of the differential aging of the human striatum. We observed significant effects of age on the neostriatal structures, whereas the paleostriatal volume was affected only in men. The magnitude of age-related neostriatal shrinkage is consistent with the estimates reported in the literature (4), and the observed pattern of aging in the globus pallidus is, to our knowledge, the first finding of this kind in healthy humans. The pattern of volume asymmetry differed across the striatal nuclei. The rightward asymmetry of the puta-

men is consistent with the trend that emerges in published studies, whereas the leftward asymmetry of the caudate is not. Finally, the lack of hemispheric asymmetry of the globus pallidus contradicts several postmortem findings (4).

The mechanisms of brain aging, in general, and of age-related changes in the striatum remain to be elucidated, and we may only speculate about possible explanations. One plausible basis for the observed pattern is a deafferentation. Both neostriatal nuclei are innervated by dopaminergic projections that arise from the substantia nigra, pars compacta (1). The source neurons of the dopaminergic afferents undergo a considerable age-related loss (21), and dopaminergic activity in the caudate nucleus is significantly reduced with age (22). Functional loss of dopaminergic receptors may progress faster than structural atrophy, at approximately 4% to 8% per decade, comparable to the age-related loss of dopamine transporters (23). Age-related degeneration of the substantia nigra may result in neostriatal atrophy, probably mediated by the loss of dopaminergic neurons. The dopaminergic deafferentation hypothesis would predict no significant shrinkage of the globus pallidus, and our finding of a lesser age effect on that structure limited only to men is consistent with this notion.

Asymmetry of the Basal Ganglia

Past research has yielded an inconsistent pattern regarding the hemispheric direction of asymmetry of the neostriatal nuclei (4). Several postmortem reports provide evidence of leftward asymmetry of the globus pallidus, whereas in vivo studies reveal an inconsistent pattern of hemispheric differences (4, 24–26). In this study, we detected a small leftward asymmetry of the caudate nucleus and a somewhat stronger asymmetry in the opposite direction in the putamen. Hemispheric differences were not detected in the volume of the globus pallidus. Asymmetries in the neostriatal structures apparently do exist in the population, but the direction of the asymmetry may vary by sample, thus yielding an inconsistent pattern of results in the literature. In addition, the consistent leftward asymmetry detected in postmortem studies of the globus pallidus may not be as readily detectable using MR imaging morphometry, in which only a part of that nucleus can be measured reliably.

Asymmetry in the neostriatum may be related to

handedness laterality and use. The predominant use of one hand could yield contralateral hypertrophy and/or ipsilateral atrophy of the striatal nuclei (27). These interpretations are concordant with the asymmetry noted in the caudate but cannot explain the findings regarding the putamen or globus pallidus.

The findings of a rightward asymmetry in the putamen and a leftward asymmetry in the caudate are commensurate with findings of higher levels of dopamine in both the right putamen and the left caudate in postmortem analyses of human brains (28). However, we did not find the pallidum to be asymmetrical, which is in contrast to the findings of Glick et al (28) of significantly higher levels of dopamine in the left globus pallidus.

Asymmetry and Aging of the Basal Ganglia

In addition to the hemispheric differences noted in the overall volumes of the neostriatal nuclei, we also found evidence of asymmetrical aging of the putamen in the full sample and of the caudate in men. While the implications of the asymmetrical aging of the putamen are unclear, greater aging of the left caudate nucleus in men may possibly be pathologic in nature. Data from perinatal research indicate that the left cerebral ventricle abutting the left caudate nucleus is more vulnerable to perinatal insult. Furthermore, left-sided perinatal insult is more prevalent in men than in women (29). Therefore, an insult involving the left caudate nucleus perinatally possibly may render the left caudate nucleus of men more susceptible to deterioration in later life. Loopuijt and Villablanca (30) found that prenatal lesions in frontal or parietal areas resulted in a significant increase in the volume of the ipsilateral caudate nucleus in cats. Thus, early insult may result in a reduction in developmental necrosis (30) and in a greater vulnerability later in life.

Methodological Limitations

The findings reported here should be viewed in the context of several methodological limitations. One drawback of the in vivo MR imaging methods used in the current study is that they cannot provide clues to the underlying cellular mechanisms of an age-related loss in volume. Losses of neuronal bodies, decreases in their volume, or decreases in dendritic arborization are all potential sources of volume reduction. Another limitation stems from the difficulty in measuring the globus pallidus. Because of the poor contrast between its anterior parts and the surrounding parenchyma, a truncated volume estimate had to be derived. Also, we were unable to separate the globus pallidus into its external and internal segments, which may be functionally and neurochemically distinct (31). Thus, our estimate of the pallidal volume, although a highly reliable and precise one, may be a less valid reflection of the structure than are the estimates for the neostriatal nuclei.

Because of reliance on the cross-sectional design, we were not able to control for the influence of cohort

effects and secular trends in brain and body size (32) on our volumetric indexes. However, covarying height extracted a large amount of the variance that might have been attributable to a secular trend. Additionally, cohort effects would have most likely resulted in a generalized pattern, rather than the observed differential reductions.

Finally, the criteria used to select subjects for this study limit the generalizability of our findings. Our sample was composed only of persons who were reportedly free of common age-associated pathologic conditions. Moreover, subjects in whom signs of mild cerebrovascular abnormalities were detected were also excluded from the data analysis. Thus, our sample is not representative of the patient population typically seen by a geriatric practitioner. We are able to conclude, however, that whatever their source, age-related differences in the volume of the basal ganglia are unlikely to stem from cerebrovascular changes commonly observed in the white matter of the elderly. In addition, because men seem to be at greater risk for age-related diseases, the men who participated in this study possibly were more atypically healthy than the women participants. Such a selection bias may have attenuated sex differences in aging trends.

Conclusion

The results of this study replicate and extend the findings of bilateral age-related shrinkage of the striatum. The pattern of observed results need to be examined in the context of neurochemical changes with age. The relative contributions of environmental and genetic factors also should be assessed. Finally, cognitive and behavioral implications of these findings need to be elucidated in future studies.

References

- Alheid GE, Switzer RC III, Heimer, L. **Basal ganglia.** In: Paxinos GT, ed. *The Human Nervous System*. San Diego: Academic Press; 1990:438-532
- Harrington DL, Haaland KY. **Skill learning in the elderly: diminished implicit and explicit memory for motor sequencing.** *Psychol Aging* 1992;7:425-434
- Mortimer JA. **Human motor behavior and aging.** *Ann N Y Acad Sci* 1988;515:54-65
- Raz N, Torres IJ, Acker JD. **Age, gender, and hemispheric differences in human striatum: a quantitative review and new data from in vivo MRI morphometry.** *Neurobiol Learn Mem* 1995;63:133-142
- Eaton WO, Reid Enns L. **Sex differences in human motor activity level.** *Psychol Bull* 1986;100:19-28
- Ward JP, Hopkins WD. *Primate Laterality: Current Behavioral Evidence of Primate Asymmetries*. New York: Springer; 1993
- Blessed G, Tomlinson BE, Roth M. **The association between quantitative measures of dementia and senile change in the cerebral grey matter of elderly subjects.** *Br J Psychiatry* 1968;114:797-811
- Radloff LS. **The CES-D scale: a self-report depression scale for research in the general population.** *Appl Psychol Meas* 1977;1:385-401
- Fazekas F, Kleinert R, Offenbacher H, et al. **Pathological correlates of incidental white matter signal hyperintensities.** *Neurology* 1993;43:1683-1689
- Schenker C, Meier D, Wichman W, Boesiger P, Valvanis A. **Age distribution and iron dependency of the T2 relaxation time in the globus pallidus and putamen.** *Neuroradiology* 1993;35:119-124
- DeCarli C, Murphy DGM, Tranh M, et al. **The effect of white**

- matter hyperintensity volume on brain structure, cognitive performance, and cerebral metabolism of glucose in 51 healthy adults. *Neurology* 1995;45:2077-2084
12. Oldfield RC. The assessment and analysis of handedness. *Neuropsychologia* 1971;9:97-113
 13. Raz N, Dupuis JH, Briggs SD, McGavran C, Acker JD. Differential effects of age and sex on the cerebellar hemispheres and the vermis: a prospective MR study. *AJNR Am J Neuroradiol* 1998;19:65-71
 14. Raz N, Gunning FM, Head D, et al. Selective aging of the human cerebral cortex observed in vivo: differential vulnerability of the prefrontal gray matter. *Cereb Cortex* 1997;7:268-282
 15. Uylings HB, van Eden CG, Hoffman MA. Morphometry of size/volume variables and comparison of their bivariate relations in the nervous system under different conditions. *Neurosci Methods* 1986;18:19-37
 16. Shrout PE, Fleiss JL. Intraclass correlations: uses in assessing raters reliability. *Psychol Bull* 1990;86:420-428
 17. Damasio H. *Human Brain Anatomy in Computerized Images*. New York: Oxford University Press; 1995
 18. De Armond SJ, Fusco MM, Dewey MM. *Structure of the Human Brain: A Photographic Atlas*. New York: Oxford University Press; 1976
 19. Nieuwenhuys R, Voogd J, van Huijzen C. *The Human Central Nervous System: A Synopsis and Atlas*. Berlin: Springer; 1988
 20. Steiger JH. Tests for comparing elements of a correlation matrix. *Psychol Bull* 1990;87:245-251
 21. Morgan DG, Finch CE. Dopaminergic changes in the basal ganglia: a generalized phenomenon of aging in mammals. *Ann N Y Acad Sci* 1988;515:145-160
 22. Goldman-Rakic PS, Brown RM. Regional changes in monoamines in cerebral cortex and subcortical structures of aging rhesus monkeys. *Neuroscience* 1981;6:177-187
 23. Volkow ND, Wang GJ, Fowler JS, et al. Measuring age-related changes in dopamine D₂ receptors with ¹¹C-raclopride and ¹⁸F-N-methylspiroperidol. *Psychiatry Res* 1996;67:11-16
 24. Castellanos FX, Giedd JN, Hamburger SD, et al. Brain morphometry in Tourette's syndrome: the influence of comorbid attention-deficit/hyperactivity disorder. *Neurology* 1996;47:1581-1583
 25. Frazier JA, Giedd JN, Hamburger SD, et al. Brain anatomic magnetic resonance imaging in childhood-onset schizophrenia. *Arch Gen Psychiatry* 1996;56:617-624
 26. Giedd JN, Snell JW, Lange N, et al. Quantitative magnetic resonance imaging of human brain development: ages 4-18. *Cereb Cortex* 1996;6:551-560
 27. Peterson B, Riddle MA, Cohen DJ, Katz LD, Smith BA, Leckman JF. Human basal ganglia volume asymmetries on magnetic resonance images. *Magn Reson Imaging* 1993;11:493-498
 28. Glick SD, Ross DA, Hough LB. Lateral asymmetry of neurotransmitters in the human brain. *Brain Res* 1982;234:53-63
 29. Raz S, Goldstein R, Shah F, et al. Sex differences in neonatal vulnerability to cerebral injury and their neurodevelopmental implication. *Psychobiology* 1994;22:244-253
 30. Loopuijt LD, Villablanca JR. Increase in size of the caudate nucleus of the cat after a prenatal neocortical lesion. *Dev Brain Res* 1993;71:59-68
 31. Afifi AK. Basal ganglia: functional anatomy and physiology. Part I. *J Child Neurol* 1994;9:249-260
 32. Miller AKH, Corsellis JAN. Evidence for a secular increase in human brain weight during the past century. *Ann Human Biol* 1977;4:253-257